GEOPHYSICS, VOL. 49, NO. 2 (FEBRUARY 1984); P. 124–131, 8 FIGS.

Migration of seismic data by phase shift plus interpolation

Jeno Gazdag* and Piero Sguazzero‡

ABSTRACT

Under the horizontally layered velocity assumption, migration is defined by a set of independent ordinary differential equations in the wavenumber-frequency domain. The wave components are extrapolated downward by rotating their phases. This paper shows that one can generalize the concepts of the phase-shift method to media having lateral velocity variations. The wave extrapolation procedure consists of two steps. In the first step, the wave field is extrapolated by the phase-shift method using ℓ laterally uniform velocity fields. The intermediate result is ℓ reference wave fields. In the second step, the actual wave field is computed by interpolation from the reference wave fields. The phase shift plus interpolation (PSPI) method is unconditionally stable and lends itself conveniently to migration of three-dimensional data. The performance of the methods is demonstrated on synthetic examples. The PSPI migration results are then compared with those obtained from a finite-difference method.

INTRODUCTION

Migration is the process of constructing the reflector surface from the recorded seismic data. In a typical sequence of processing steps, the normal moveout (NMO) correction is applied first to a set of common midpoint (CMP) gathers. By summing these gathers over offset, one obtains a CMP stack. NMO correction and stacking is a process whereby the waves are shifted along the offset axis toward the zero offset. Therefore, a CMP stack is normally migrated as a zero-offset section.

Seismic migration consists of two steps: (1) wave extrapolation and (2) imaging. Downward extrapolation results in a wave field that is an approximation to the one that would have been recorded if both sources and recorders had been located at depth z. In the case of zero-offset data, imaging consists of mapping the data from zero time ($t = 0$) of the time section to the proper depth of the migrated section.

Since imaging is a trivial task, migration schemes differ in their approach to the wave extrapolation problem, whose complexity depends largely on the migration velocity function. If the migration velocity has no horizontal variations, the extrapolation of the recorded seismic data can be expressed by an exact wave-extrapolation equation in the wavenumber-frequency domain. This equation has a simple analytic solution, whose implementation calls for a phase shift applied to the Fourier coefficients of the zero-offset section.

In the presence of lateral velocity variations, the exact wave-extrapolation equation is no longer valid. To circumvent this problem, the exact expression can be approximated by some series expansion (Hatton et al, 1981; Claerbout, 1980; Gazdag, 1980), which can accommodate horizontal velocity variations. These equations are then solved numerically, either in the space-time domain or in the space-frequency domain. Finite-difference migration methods formulated in the space-time domain or in the space-frequency domain are characterized by some of the following properties: (1) inaccurate dispersion relations for steep dips, (2) numerical errors resulting from the finite-difference approximation used, and (3) predisposition to numerical instability. The stability problem is kept under control by using implicit methods, which are also reasonably accurate and economical for two-dimensional (2-D) data. However, Claerbout (1980) finds that "in space dimensions higher than one the implicit method becomes prohibitively costly."

The aim of this paper is to develop a migration scheme whose cost and complexity do not depend significantly on the dimensionality of the data. In other words, the desired migration scheme is one that has no problems with higher dimensions. Another important goal is that the method be unconditionally stable. It may seem like a fortuitous coincidence that the wave-extrapolation algorithm that achieves the above objectives is also accurate. The wave extrapolation with a laterally varying velocity field consists of two steps. In the first step, the wave field is extrapolated by the phase-shift method (Gazdag, 1978), using ℓ laterally uniform velocity fields. The intermediate result is ℓ reference wave fields. In the second step, the actual wave field is computed by interpolation from the reference wave fields.

The organization of this paper is as follows. The first section is a review of the basic theory, and a description of a finite-

Manuscript received by the Editor April 19, 1983; revised manuscript received August 2, 1983.
*IBM Scientific Center, 1530 Page Mill Road, Palo Alto, CA 94304.
‡IBM Scientific Center, Via del Giorgione 129, Rome, Italy.

difference migration (FDM) method is given. Next the phase shift plus interpolation (PSPI) method is presented. This is followed by testing the PSPI method. Synthetic zero-offset sections are migrated by the FDM and the PSPI algorithms to contrast their performance. Finally, the migration results are discussed.

WAVE EXTRAPOLATION EQUATIONS

This section reviews the basic concepts of wave-extrapolation theory. The aim is to provide the reader with the background information to the PSPI method and the motivating reasons for its development. The simple case of depth-variable velocity is presented first. The treatment of laterally varying velocities is taken up next. This is followed by a description of a finite-difference migration method which serves as a means of comparison in the performance test of the PSPI method.

Depth-variable velocity

The theory of wave extrapolation is based on the assumption that the zero-offset pressure data, defined in the (x, t) domain, satisfy the scalar wave equation

$$\frac{\partial^2 p}{\partial z^2} = \frac{1}{v^2}\frac{\partial^2 p}{\partial t^2} - \frac{\partial^2 p}{\partial x^2} \tag{1}$$

with $p = p(x, z, t)$, where x is the midpoint variable, z is depth, t is two-way traveltime, and v is the half velocity. To obtain a better understanding of equation (1), it is helpful to express p as a double Fourier series

$$p(x, z, t) = \sum_{k_x}\sum_{\omega} P(k_x, z, \omega)\exp\left[i(k_x x + \omega t)\right], \tag{2}$$

where k_x is the midpoint wavenumber and ω is the temporal frequency. Substituting equation (2) into equation (1), one obtains

$$\frac{\partial^2 P}{\partial z^2} = -k_z^2 P, \tag{3}$$

which has an analytic solution

$$P(k_x, z + \Delta z, \omega) = P(k_x, z, \omega)\exp\left(ik_z \Delta z\right) \tag{4}$$

for each k_z, where k_z can be expressed as

$$k_z = \pm\frac{\omega}{v}\left[1 - \left(\frac{vk_x}{\omega}\right)^2\right]^{1/2} \tag{5}$$

in order to differentiate between two classes of solutions. In a downward extrapolation process, i.e., when Δz in equation (4) is positive, sign agreement between k_z and ω corresponds to waves that move in the negative t direction. On the other hand, when k_z and ω have opposite signs, equation (4) represents waves that move in the positive t direction. Since the downward extrapolation of recorded seismic data is an inverse process, one is interested only in

$$k_z = \frac{\omega}{v}\left[1 - \left(\frac{vk_x}{\omega}\right)^2\right]^{1/2}, \tag{6}$$

which corresponds to waves moving in the reverse-time direction.

It should be noted that the choice of sign in equation (5) does not differentiate between upcoming and downgoing waves. This is decided by the sign of Δz in equation (4). Downward extrapolation requires that Δz be greater than zero. Once Δz is set, the two values of k_z in equation (5) correspond to forward-time and reverse-time wave propagation. Substituting equation (6) into equation (4), one obtains the desired expression for wave extrapolation

$$P(k_x, z + \Delta z, \omega) = P(k_x, z, \omega)\exp\left\{\frac{i\omega}{v}\left[1 - \left(\frac{k_x v}{\omega}\right)^2\right]^{1/2}\Delta z\right\}. \tag{7}$$

One can verify by inspection that equation (7) is the solution of

$$\frac{\partial P(k_x, z, \omega)}{\partial z} = i\left(\frac{\omega}{v}\right)\left[1 - \left(\frac{k_x v}{\omega}\right)^2\right]^{1/2} P(k_x, z, \omega), \tag{8}$$

which is the exact extrapolation equation for constant velocity. Velocity variations with respect to the depth variable are accommodated easily by simply varying the velocity with z in equation (7).

Lateral velocity variations

The simple analytic solution expressed by equation (7), which is the basis of the phase-shift method, is not valid for velocity fields with lateral variations. In this case, the square root expression in equation (8) is usually expanded into some kind of truncated series. The Taylor series expansion of equation (8) can be developed into an accurate numerical method in the (x, ω) domain (Gazdag, 1980). Another alternative is approximation by continued fractions (Hildebrand, 1956, p. 422). This approach to developing wave extrapolators was first suggested by Francis Muir (Claerbout, 1980). The idea is to expand

$$R = (1 - K^2)^{1/2} \tag{9}$$

based on the recurrence relation

$$R_{n+1} = 1 - \frac{K^2}{1 + R_n}, \tag{10}$$

in which R_n is the nth order approximation. To show that this expansion converges to equation (9), one needs only to substitute $n = \infty$ into equation (10). Starting out with $R_0 = 1$, one obtains

$$R_1 = 1 - \frac{K^2}{2} \tag{11}$$

and

$$R_2 = 1 - \frac{K^2}{2 - \frac{1}{2}K^2}. \tag{12}$$

Approximating the square root expression by R_2 and substituting it into equation (6) with

$$K = k_x v/\omega, \tag{13}$$

one obtains

$$k_z = \frac{\omega}{v} - \frac{k_x^2}{2\omega/v - k_x^2 v/2\omega}. \tag{14}$$

Similarly, the second-order approximation of equation (8) becomes

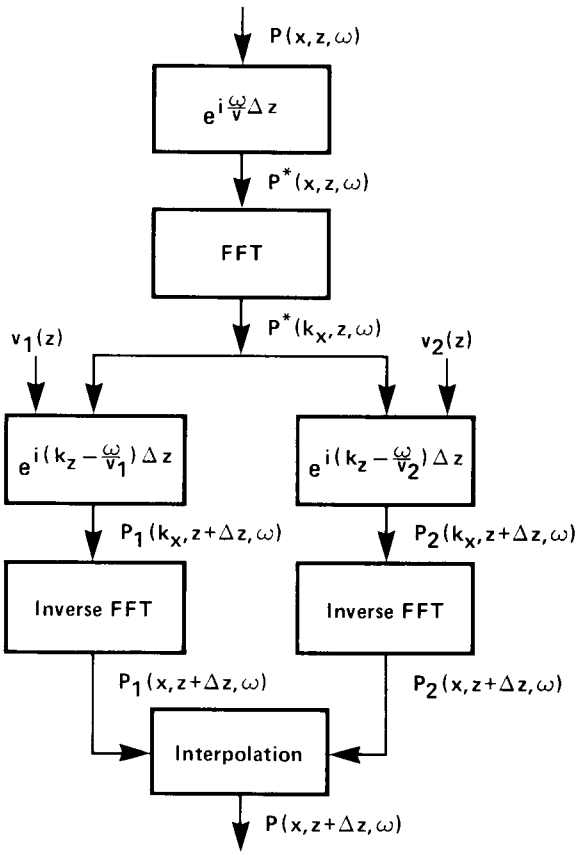

FIG. 1. Computational diagram of the PSPI extrapolation scheme corresponding to equations (25) and (26).

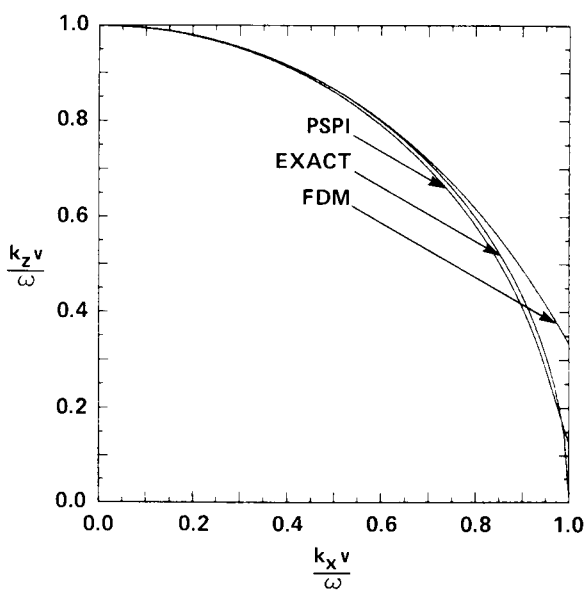

FIG. 2. Dispersion relations for the finite-difference method [equation (14)] and the PSPI method [equation (37)]. For comparison the exact dispersion relations corresponding to equation (6) are also shown. The PSPI curve refers to velocity $v = 1.25v_1$ with reference velocities v_1 and $v_2 = 1.5v_1$.

$$\frac{\partial P}{\partial z} = i\left[\frac{\omega}{v} - \frac{(v/2\omega)k_x^2}{1-(k_x v/2\omega)^2}\right]P. \tag{15}$$

A finite-difference extrapolator in the (x, ω) domain

A practical approach to solving extrapolation equations like equation (15) is by splitting. This is done by decomposing equation (15) into two extrapolators:

$$\frac{\partial P}{\partial z} = \frac{i\omega}{v}P \tag{16}$$

and

$$\frac{\partial P}{\partial z} = \frac{-i(v/2\omega)k_x^2}{1-(k_x v/2\omega)^2}P. \tag{17}$$

Advancing to greater depths is done by applying equations (16) and (17) alternately in small Δz steps. To express equation (17) in the (x, ω) domain, it is first multiplied by the denominator of its right-hand side, and then both sides are Fourier transformed with respect to k_x. The result is

$$\left[1+\left(\frac{v}{2\omega}\right)^2 D_{xx}\right]D_z P = \frac{iv}{2\omega}D_{xx}P, \tag{18}$$

in which D_{xx} and D_z signify partial derivatives with respect to x and z. Migration by means of equations (16) and (18) was first reported by Kjartansson (1978). In this equation, velocity dependence need not be restricted to the depth variable alone, but it may also include lateral variations.

Equation (18) is solved numerically by means of approximating it with a set of algebraic equations involving the values of P at the grid points (j, n). If Δx is the grid spacing and Δz is the integration step, then the indices j and n refer to $x = j\Delta x$ and $z = n\Delta z$, respectively. To simplify notations in the finite-difference formulation, the wave field at grid point (j, n) will be denoted as $P_{j,n}$, where

$$P_{j,n} = P(j\Delta x, n\Delta z, \omega). \tag{19}$$

If the differential operators are approximated as

$$D_z P_{j,n+1/2} = (P_{j,n+1} - P_{j,n})/\Delta z \tag{20}$$

and

$$D_{xx}P_{j,n} = (P_{j-1,n} - 2P_{j,n} + P_{j+1,n})/\Delta x^2, \tag{21}$$

the finite-difference approximation of equation (18) becomes

$$P_{j,n+1} + (\alpha - i\beta)(P_{j-1,n+1} - 2P_{j,n+1} + P_{j+1,n+1}) = P_{j,n} + (\alpha + i\beta)(P_{j-1,n} - 2P_{j,n} + P_{j+1,n}), \tag{22}$$

where

$$\alpha = \left(\frac{v}{2\omega\Delta x}\right)^2$$

and

$$\beta = \frac{v\Delta z}{4\omega\Delta x^2}. \tag{23}$$

Equation (22), for $j = 1, 2, \ldots, N_x$, represents a system of linear differential equations with complex coefficients. This system of equations is then solved for all ω values, and the migrated data at $z + \Delta z$ are obtained by

$$p(x, z + \Delta z, t = 0) = \sum_{\omega} P(x, z + \Delta z, \omega), \tag{24}$$

where the summation is carried out for all ω values. The implementation of equation (24) represents the imaging step of the migration process. In what follows, the migration technique described above will be referred to as FDM. In the Fortran program of the FDM scheme which is used in the migration examples of this paper, the system of equations (22) involving a complex tridiagonal matrix is solved by using the subroutine CJTSL of LINPACK (Dongarra et al, 1979).

The wave-extrapolation method described above has been formulated in the (x, ω) domain. Starting with equation (18), or its inverse Fourier transform with respect to ω, one can also develop finite-difference solution methods in the (x, t) domain. The main advantage of the (x, ω) domain approach is that numerical errors due to time differencing are eliminated.

MIGRATION BY PHASE SHIFT PLUS INTERPOLATION

Under the horizontally layered velocity assumption, the phase-shift method expressed by equation (7) has considerable advantage over extrapolators expressed in the (x, t) and the (x, ω) domains. Its accuracy is due to exact dispersion relations [equation (6)] and the existence of a simple analytic solution to equation (8). The numerical implementation of equation (7) is unconditionally stable in both two and three dimensions. These attractive qualities provide ample motivation for inquiring into the possibilities of generalizing the phase-shift method to laterally varying velocities.

The PSPI extrapolation method has been developed to meet this objective. This procedure is centered around the idea that lateral velocity variations can be taken into account by interpolation among wave fields that were downward-continued by phase shift, using two or more reference velocities. Since the concepts are not altered by the number of reference velocities, the PSPI extrapolation scheme will be discussed for the two-velocity case, the computational diagram of which is shown in Figure 1.

To maintain high accuracy for small dips, when $k_x v/\omega \ll 1$, the phase shift expressed in equation (4) is split into two distinct operations:

$$P^*(z) = P(z) \exp\left(i \frac{\omega}{v} \Delta z\right) \tag{25}$$

and

$$P(z + \Delta z) = P^*(z) \exp\left[i\left(k_z - \frac{\omega}{v'}\right)\Delta z\right], \tag{26}$$

where $v' \neq v(x, z)$ is an approximation to $v(x, z)$ as outlined below. Equation (25) is a time shift applied to each trace. This algorithm involves no numerical approximations in the (x, ω) domain. Since equation (26) cannot be computed directly when $v = v(x, z)$, its implementation is approximated in several steps shown in Figure 1. First P^* is Fourier transformed with respect to x. This is followed by the phase-shift operation expressed in equation (26) using two velocities, v_1 and v_2, which are defined as the extrema of $v(x, z)$:

$$v_1(z) = \text{Min } [v(x, z)]$$

and (27)

$$v_2(z) = \text{Max } [v(x, z)].$$

The phase-shifted wave fields $P_1(k_x, z + \Delta z, \omega)$ and $P_2(k_x, z + \Delta z, \omega)$ are then inverse transformed, resulting in the reference wave fields $P_1(x, z + \Delta z, \omega)$ and $P_2(x, z + \Delta z, \omega)$, which serve as reference data from which the final result $P(x, z + \Delta z, \omega)$ is obtained by interpolation in the following manner. First, the Fourier coefficients are expressed in terms of their modulus and phase angle:

$$P_1(x, z + \Delta z, \omega) = A_1 \exp(i\theta_1) \tag{28}$$

and

$$P_2(x, z + \Delta z, \omega) = A_2 \exp(i\theta_2). \tag{29}$$

Second, the modulus and phase of the end result are obtained by means of linear interpolation:

$$A = \frac{A_1(v_2 - v) + A_2(v - v_1)}{v_2 - v_1} \tag{30}$$

and

$$\theta = \frac{\theta_1(v_2 - v) + \theta_2(v - v_1)}{v_2 - v_1}, \tag{31}$$

from which one can write

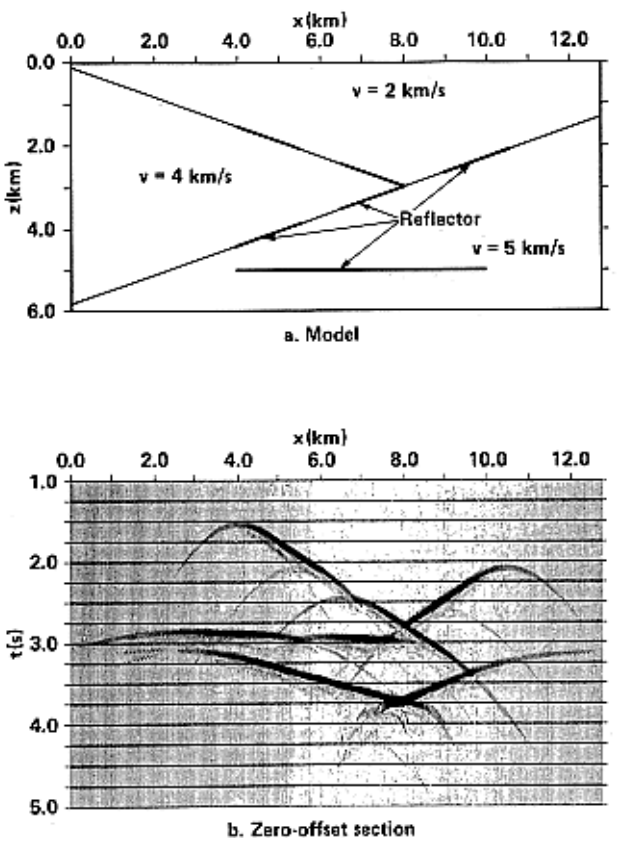

FIG. 3. (a) Schematic of model 1, representing a dipping multilayer example. The thick-line segments denote where the reflector segments have been "turned on." (b) Synthetic zero-offset time section of model 1.

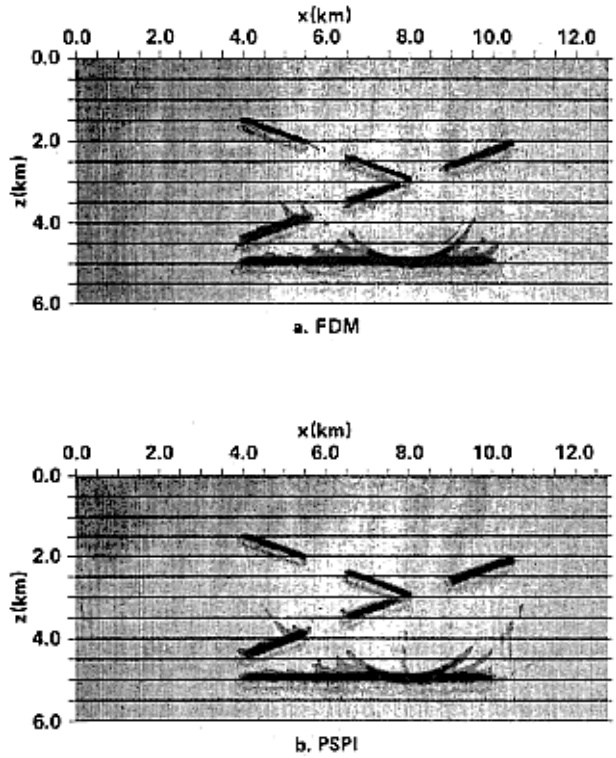

FIG. 4. Depth migration sections obtained from the zero-offset section shown in Figure 3b by means of (a) the finite-difference method (FDM) and (b) the PSPI method.

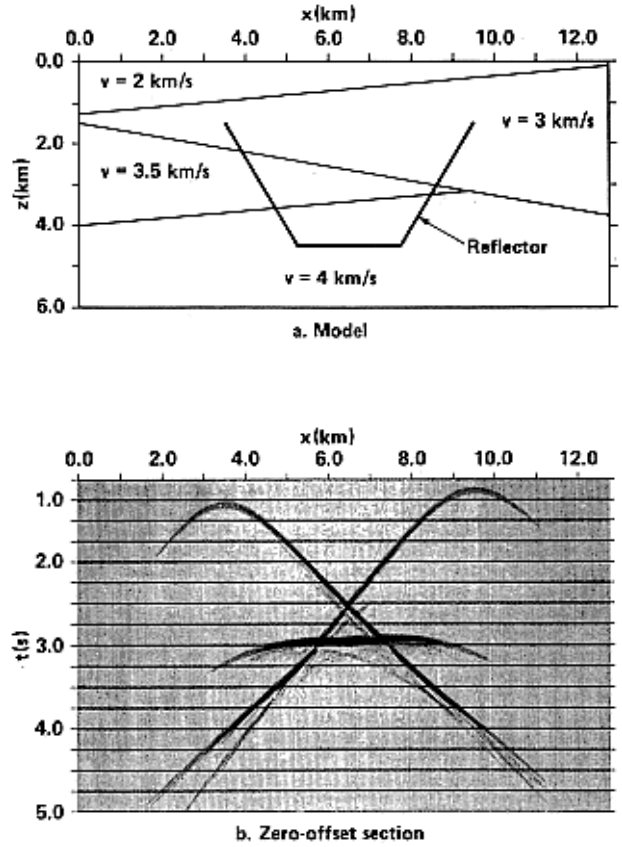

FIG. 5. (a) The aim of model 2 is to illustrate the performance of the two migration schemes for reflectors with 60-degree dips in a dipping multilayer medium. (b) Synthetic zero-offset time section of model 2.

$$P(x, z + \Delta z, \omega) = A \exp(i\theta). \tag{32}$$

Definition of k_z

To obtain $\theta = (k_z - \omega/v)\Delta z$ in equation (26) by interpolation over the domain

$$-1 \le k_x v/\omega \le 1, \tag{33}$$

the reference phase angle θ_2 must be specified over a domain that is v_2/v times greater. To accommodate any velocity v such that $v_1 \le v \le v_2$, the vertical wavenumber k_z should be defined over the domain

$$-v_2/v_1 \le k_x v/\omega \le v_2/v_1. \tag{34}$$

It should be noted that k_z has no physical significance outside of the domain given by equation (33). The need for the extended domain is to obtain satisfactory interpolated phase angles for $k_x v/\omega$ that satisfy equation (33).

Depending upon v_2/v_1 and other considerations such as the extrema (Nyquist) of k_x, there are many ways of continuing k_z beyond the limits set in equation (33). One solution, which is by no means an optimal choice with respect to any particular criterion, to be considered in this paper is the following:

$$k_z = \frac{\omega}{v}(1 - K^2)^{1/2} \qquad \text{for} \quad 0 \le |K| \le 0.95, \tag{35}$$

$$k_z = \frac{\omega}{v}[0.312 - 3.042(|K| - 0.95)] \quad \text{for} \quad 0.95 \le |K| \le 1.5,$$

where $K = k_x v/\omega$ and $v_2 \le 1.5v_1$. In this definition, k_z matches the exact square root expression up to $k_x v/\omega = 0.95$, which corresponds to 71.8 degree dip. From there it is continued along the tangent drawn at that point.

Accuracy of interpolation

The interpolation accuracy depends upon the ratio of the reference velocities (v_2/v_1) and the actual migration velocity $v(x)$. The effective phase rotation resulting from the PSPI method shown in Figure 1 is

$$\phi = \frac{\omega}{v}\Delta z + \theta, \tag{36}$$

in which the two terms correspond to the contributions from equations (25) and (26). By setting Δz to unity and multiplying both sides by v/ω, one obtains

$$\left(\frac{k_z v}{\omega}\right) = 1 + \theta\frac{v}{\omega}. \tag{37}$$

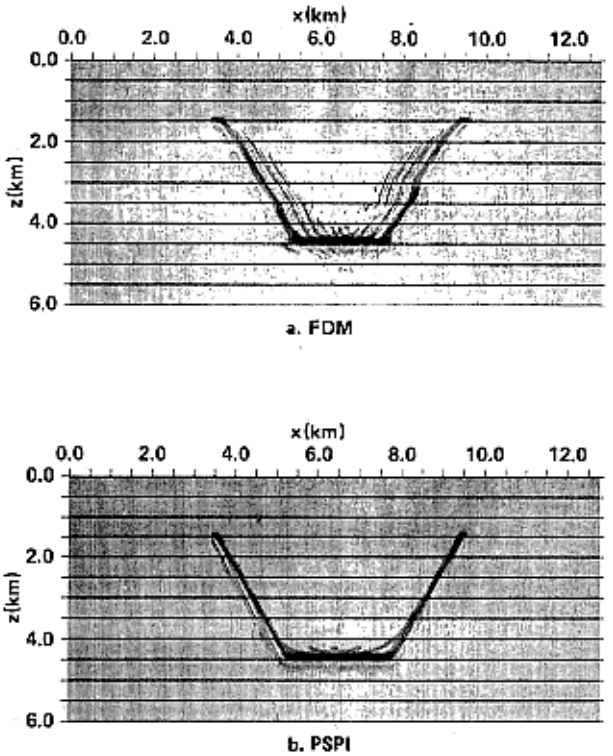

FIG. 6. Depth migration sections obtained from the zero-offset section shown in Figure 5b by using (a) the finite-difference method (FDM) and (b) the PSPI method. The steeply dipping events are smeared by the FDM migration but suffer no such distortion from the PSPI method.

By expressing θ as the function of $k_x v/\omega$, one can calculate and plot the dispersion relations, $k_z v/\omega$ versus $k_x v/\omega$, for the velocity range under consideration.

Figure 2 shows three dispersion relations corresponding to (1) the exact phase shift expressed in equation (6), (2) the FDM 45-degree algorithm characterized by equation (14), and (3) the PSPI method as described above. The latter result applies to the $v_2/v_1 = 1.5$ case. Moreover, the velocity of interpolation $v = 1.25v_1$ is in the middle of the (v_1, v_2) interval, and hence it falls in the least accurate velocity range. By contrast, as v approaches either v_1 or v_2, the PSPI dispersion relation curve approaches the exact curve up to $k_x v/\omega = 0.95$, or equivalently, 71.8-degree dips.

Choice of reference velocities

Up to now the number of reference velocities was limited to two, in order to facilitate the description of the ideas. When at some depth $z = z'$ the ratio of Max $[v(x, z')]$ and Min $[v(x, z')]$, which will be referred to as R, exceeds some upper bound, say $\rho_{max} = 1.5$, more than two reference velocities are needed. The number of reference velocities ℓ required is obtained as the smallest integer for which

$$(\rho_{max})^{\ell-1} \geq R. \tag{38}$$

Then the consecutive reference velocities are chosen to form a geometric progression $v_{i+1}/v_i = v_i/v_{i-1} = \rho$ for $2 \leq i \leq \ell - 1$, where $(\rho)^{\ell-1} = R$. If ℓ is greater than 2, the interpolation expressed in equations (30) and (31) is performed by using the reference velocities that are closest to the velocity of the medium $v(x, z)$.

SYNTHETIC EXAMPLES

To test the reliability of the PSPI method and compare its performance with the FDM algorithm, three synthetic zero-offset sections were migrated with both methods. The aim was to determine the sensitivity of migration accuracy to steep dips and lateral velocity variations. In each example the zero-offset section is defined over a grid of size $N_x \times N_t$, with $N_x = 256$ and $N_t = 256$. The grid spacings are $\Delta x = 50$ m and $\Delta t = 50$ msec. The integration step is $\Delta z = 50$ m.

The synthetic zero-offset sections are generated by simulating reflectors as an ensemble of point scatterers. The computer implementation of this method is essentially based upon Huygens' construction. To obtain the zero-offset section of an elementary diffractor, rays are traced in every direction through the medium up to the surface. A wavelet whose amplitude is proportional to the strength of the diffractor is assigned (after taking into account geometrical spreading effects) to the grid point of the time section corresponding to the arrival of the ray at the surface. The contributions of all point diffractors are then summed to obtain the zero-offset section of the structure.

Figure 3 shows the schematic and zero-offset section of model 1. The reflectors are indicated by means of thick lines to distinguish them from interfaces of velocity regions depicted by thin lines. Figure 4 shows the migrated results of model 1 obtained by the FDM and the PSPI methods. This model has modest velocity variations and dip angles, and therefore, it does not present much challenge to either method. The situation is quite different in the case of model 2, shown in Figures 5 and 6, which aims to test the ability of the methods to migrate steeply dipping events. The reflectors situated on the two sides form 60-degree dips with respect to the horizontal axis. While the reflectors in model 3 are horizontal, the challenge is in coping with a velocity ratio of 2.5 along the interface shown in Figure 7, part of which is directed at 60 degrees with respect to the horizontal axis.

DISCUSSION OF RESULTS

The migrated depth sections of model 1 shown in Figure 4 are of similar overall quality. There are small differences in the three top reflectors, all of which are located at the lower boundary of the $v = 2$ km/sec velocity region. These events are better migrated by the PSPI method. A noteworthy feature of the migrated sections shown in Figures 4a and 4b is a circular pattern extending down to the $z = 5$ level. The similarity between these phenomena in the two sections (FDM and PSPI) rules out the possibility that they might be of numerical origin. Detailed study of the origin of these patterns indicates that they are diffracted waves originating from the neighborhood of $(x = 8, z = 3)$, where the $v = 4$ km/sec velocity region narrows to a point.

The migrated sections of model 2 (Figure 6) demonstrate the superiority of the PSPI over the FDM for migration of events having 60 degree dips. The FDM results are dispersed, and the

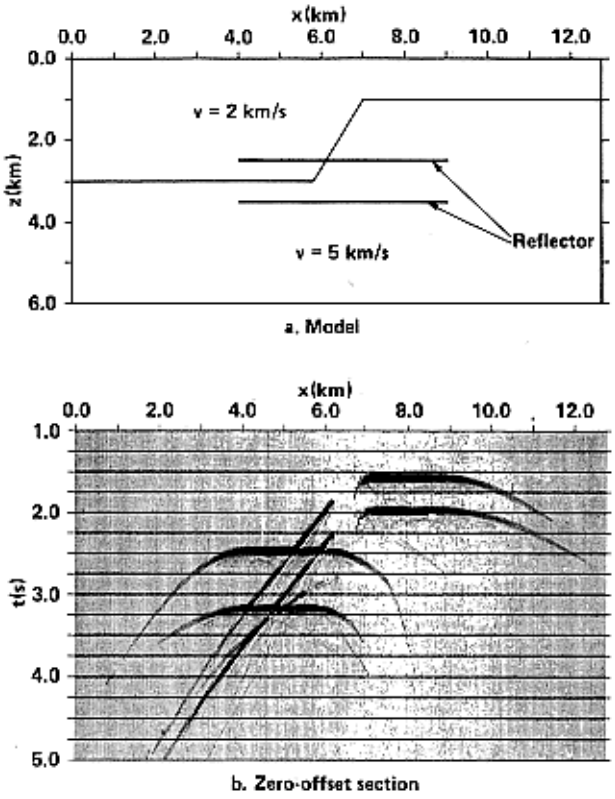

FIG. 7. (a) Model 3 is intended to test the performance of the two migration schemes in the presence of strong lateral velocity variations. (b) Synthetic zero-offset time section of model 3.

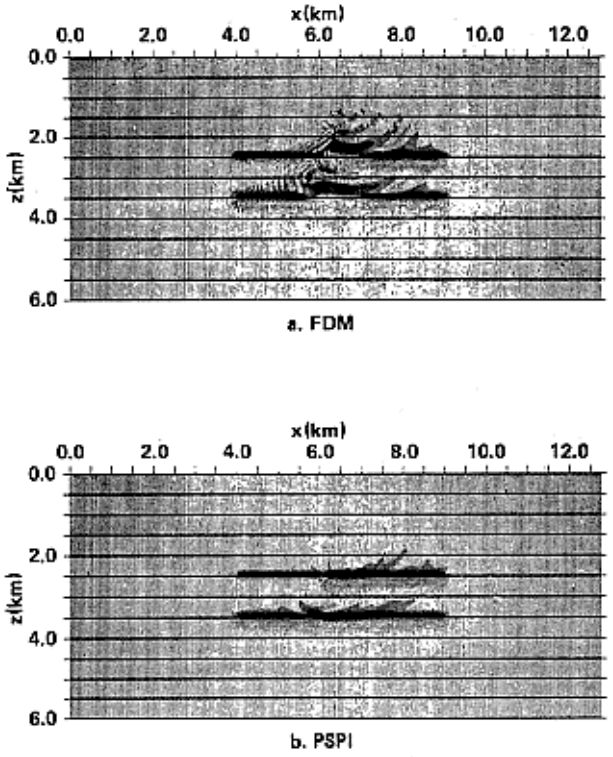

FIG. 8. Depth migration sections obtained from the zero-offset section shown in Figure 7b with (a) the finite-difference method and (b) the PSPI method. The PSPI scheme results in better images of the two horizontal reflectors.

reflector appears to have a break in the vicinity of ($x = 8.5$, $z = 3$), where it traverses the $v = 3.5$ km/sec region.

Model 3 tests the sensitivity of migration accuracy to strong velocity variations. The two horizontal reflectors are imbedded in a medium having a sudden velocity change along an interface directed 60 degrees with respect to the x axis (Figure 7a). In the zero-offset section each reflector results in three distinct recorded images (Figure 7b). Whereas the reconstruction of the horizontal reflectors shown in Figure 8 is not completely satisfactory with either case, the PSPI result is significantly better than the one obtained by FDM. The left-hand side of the upper reflector imbedded in the $v = 2$ km/sec region is weaker than its remaining part. This is due to the particular nature of the modeling program, which takes into account amplitude attenuation due to geometric spreading as a function of time $(t)^{1/2}$ rather than as a function of distance $(r)^{1/2}$. Consequently, the attenuation is exaggerated for waves traveling in low-velocity regions relative to those propagating in higher velocity media.

An ideal wave extrapolator, while restricting propagation in the reverse-time direction, is expected to simulate wave phenomena to a limited extent. Waves being extrapolated in a medium having sudden velocity changes are subject to sideways reflections, and in the case of sharp corners such as in model 1, the waves are scattered in a way that resembles diffraction. No attempt was made to remove such effects from the migrated results. In practice, however, such reflected and diffracted events are hardly useful at all. Fortunately, their effect can be easily minimized by choosing smooth velocities across interfaces. Perhaps the best strategy is simply to avoid sudden variations in the migration velocity. When the velocity variations are gradual, i.e., changes take place over several grid spacings instead of one, the undesirable "wave phenomena" are minimized without affecting the quality of migration.

CONCLUSIONS

It has been shown that the phase-shift plus interpolation method is a practical alternative solution to migration by finite-difference methods in the presence of lateral velocity variations. The dispersion relations of this migration method approach the exact ones in the neighborhood of the reference velocities. Consequently, as the ratio of two consecutive reference velocities approaches unity, which may be the case in regions of mild lateral velocity variations, the performance of this method approaches that of the phase-shift method. Similarly, the overall accuracy of migration increases with the number of reference velocities used. The use of more reference velocities means more computation, but the user has the option to determine the trade-off between performance and cost. Since the PSPI

method consists of the evaluation of analytic solutions followed by interpolation, the truncation errors due to finite differencing are minimized, and the question of stability never even arises. Finally, perhaps the most significant attribute of the PSPI method is that it is generally applicable to problems of any dimensionality.

REFERENCES

Claerbout, J. F., 1980, Personal communication.
Dongarra, J. J., Moler, C. B., Bunch, J. R., and Stuart, J. W., 1979, LINPACK Users' Guide: Philadelphia, SIAM, p. 7.1–7.6.
Gazdag, J., 1978, Wave equation migration with the phase-shift method: Geophysics, v. 43, p. 1342–1351.
——— 1980, Wave equation migration with the accurate space derivative method: Geophys. Prosp., v. 28, p. 60–70.
Hatton, L., Larner, K. L., and Gibson, B. S., 1981, Migration of seismic data from inhomogeneous media: Geophysics, v. 46, p. 751–767.
Hildebrand, F. B., 1956, Introduction to numerical analysis: New York, McGraw-Hill.
Kjartansson, E., 1978, Personal communication.
Robinson, E. A., and Silvia, M. T., 1981, Digital foundations of time series analysis: v. 2—Wave-equation space-time processing: San Francisco, Holden-Day, Inc.